Fish and Shellfish Immunology Reports 4 (2023) 100081

Contents lists available at ScienceDirect

Fish and Shellfish Immunology Reports

journal homepage: www.sciencedirect.com/journal/fish-and-shellfish-immunology-reports

Molecular characterization and functional analysis of peroxiredoxin 3 (NdPrx3) from *Neocaridina denticulata sinensis*

Ce Xu [a], Ying Wang [a], Ruirui Zhang [a], Jiquan Zhang [a,*], Yuying Sun [a,b,*]

[a] School of Life Sciences, Institute of Life Sciences and Green Development, Engineering Laboratory of Microbial Breeding and Preservation of Hebei Province, Hebei University, Baoding 071002, China
[b] Key Laboratory of Microbial Diversity Research and Application of Hebei Province, Hebei University, Baoding 071002, China

ARTICLE INFO

Keywords:
Peroxiredoxin
Neocaridina denticulata sinensis
Antioxidant
Stress response

ABSTRACT

Peroxiredoxins (Prxs) widely exist in organisms and can prevent oxidative damage. Here, the characterization and biological function of NdPrx3 from *Neocaridina denticulata sinensis* were analyzed. The coding sequence of *NdPrx3* consists of 684 bp open reading frame (ORF), encoding 227 amino acids with a predicted molecular weight of 24.7 kDa and theoretical pI 6.49. Multiple sequence alignments showed that the conserved domains of NdPrx3, including catalytic triad, dimer interface, decamer interface, peroxidatic, and resolving cysteines, were similar to those of other organisms. The phylogenetic relationship demonstrated that NdPrx3 clustered in the Prx3 class. The highest relative expression of *NdPrx3* mRNA was confirmed in gill among the nine tissues from healthy shrimp. The transcript level of *NdPrx3* was significantly upregulated from 0 h to 48 h and decreased in 72 h under copper challenge, indicating that *NdPrx3* may play an important role in the copper challenge of *N. denticulata sinensis*. In addition, NdPrx3 was recombinantly expressed in *E. coli* and purified to one band on SDS-PAGE. The DNA protection of rNdPrx3 was verified. The enzymatic assay of the recombinant NdPrx3 indicated that it had the oxidoreductase function and was stable at a low temperature (10–30 °C).

1. Introduction

Peroxiredoxins (Prxs) are a superfamily of cysteine-dependent peroxidases that was first identified in *Saccharomyces cerevisiae* in 1987. These proteins were initially called thiol-specific antioxidants (TSA) for their ability to reduce peroxide with thiol [1]. After several changes, it was finally named Prx [2–4]. Different from other conventional peroxidases, thiol-electron donors of conserved cysteine residues have been used as electron donors in Prxs instead of other metal irons or groups with redox functions [5].

Prxs can be divided into three groups: typical 2-Cys-Prxs, 1-Cys-Prxs, and atypical 2-Cys-Prxs. The distinct between 2-Cys-Prxs and 1-Cys-Prxs is the number of Cys-residues. 2-Cys-Prxs contain N- and C- terminal Cys-residues, but 1- Cys-Prxs only have N- terminal Cys-residues [6]. In addition, the difference between typical Prx and atypical Prx lies in the catalytic process [7]. Only Prx6 belongs to 1-Cys-Prxs of the six peroxiredoxins expressed in mammalian cells, and others can be classified into typical 2-Cys (Prx1–4) and atypical 2-Cys (Prx 5) [8].

The two conserved cysteines of typical 2-Cys-Prxs are also named "Peroxidatic Cys" (C_P) and "Resolving Cys" (C_R) for their different functions in peroxide reduction [9]. In the process of peroxide removal, C_P initially reacts with peroxide to produce sulfenic acid, C_PSOH. C_PSOH will be attacked by C_R and form a disulfide bond and H_2O in the normal catalytic cycle. Finally, this disulfide bond is broken down by thioredoxin-like molecule and regenerates C_P and C_R [10,11]. However, an additional cycle may occur because the protein regions around the active site change conformation to accept another peroxide when C_PSOH has been produced. C_PSOH will be oxidized into C_PSO_2H and then reduced by sulfiredoxin and possible sestrins under the condition with ATP [12,13].

Prx3 is primarily existed in mitochondria, being detected in the mitochondrial matrix and consuming ~90% of hydrogen peroxide produced. Mitochondria have been considered one of the main energy providers in both cells of animals and plants [14,15]. Prx3 can help mitochondria resist oxidative damage caused by reactive oxygen species (ROS) generated by aerobic respiration [16,17]. These activities of Prxs are critical to protecting normal cells from Oncogenesis. However, it is not only one mechanism of antioxidation in the process of preventing

* Corresponding authors at: School of Life Sciences, Institute of Life Sciences and Green Development, Engineering Laboratory of Microbial Breeding and Preservation of Hebei Province, Hebei University, Baoding 071002, China.
E-mail addresses: zhangjiquan@hbu.edu.cn (J. Zhang), sunyuying125@hbu.edu.cn (Y. Sun).

https://doi.org/10.1016/j.fsirep.2023.100081
Received 16 November 2022; Received in revised form 1 January 2023; Accepted 1 January 2023
Available online 4 January 2023

Table 1
Sequence of primers used in this study.

Primers	Sequences (5′ −3′)	
NdPrx3-F	TCCGCCCACCATCACCATCACCATGC AGGAATTTTGAGAAAATTC	Confirm target gene
NdPrx3-R	TCCGTAGACAGAGCATTAGTTAACTTT TTCAAAGT	Confirm target gene
NdPrx3-F0	CTTTACAACCATGGCAGGAATTTTGA	Confirm target gene
18S-F	TATACGCTAGTGGAGCTGGAA	Real-time PCR
18S-R	GGGGAGGTAGTGACGAAAAAT	Real-time PCR
NdPrx3-qF	CCAACCGAGTTAATTGCCTTCA	Real-time PCR
NdPrx3-qR	GCCTCCTTGCTTCCTTGACA	Real-time PCR

cancer. Prxs also play an important role in phosphorylation and signal transduction [18–20]. In addition, other functions of Prx3 have been characterized in many studies [21]. The selectivity of Prxs in the transduction of peroxide signals had been verified by a mass-spectrometry-based approach [22]. The DNA protection activity of Prxs was investigated in *Hippocampus abdominalis* and *Oplegnathus fasciatus* [23,24]. Previous studies of Prx3 have been reported in many aquatic organisms, including *O. fasciatus* [25], *H. abdominalis* [26], and *Cyprinus carpio* [27]. However, little is known about Prx3 in *Neocaridina denticulata sinensis*.

N. denticulata sinensis is a small size shrimp and widely distributed in freshwater ecosystems around Asia [28]. It is crucial to aquatic ecosystems because it is the mainly food resource supplied for macroinvertebrates, fish, and water birds [29,30]. It feeds primarily on residue, undesired algae and the roots of macrophytes, so this shrimp is involved in aquariums cleaners [31]. Due to the variety of colors including red, blue and yellow, *N. denticulata* has great success in the aquarium market as an ornamental shrimp [32]. Comprehensive analysis of the characteristics of *N. denticulata* such as growth rate, reproductive ability and vitality [33,34], this shrimp has the potential to become a model for studying crustaceans [28]. Here, the NdPrx3 from *N. denticulata sinensis*, belonging to Prx3 subfamily, was characterized at the molecular level and its functional activities were also analyzed.

2. Materials and methods

2.1. Experimental animal, the challenge experiment and tissue extraction

The shrimp used in this experiment were purchased from a local aquaculture center in Anxin County, Baoding, Hebei Province. All of the shrimp were acclimated for 30 days in blue plastic tanks (70 cm × 50 cm × 40 cm). During the feeding trial, shrimp were fed with a commercial diet at 4% of body weight once a day, and the residual feed was cleared two hours later. 10% water was replaced every day with fresh water. The temperature was maintained at 25.0 ± 1.0 °C.

After acclimation, nine tissues (cuticle, eyestalk, muscle, intestine, hepatopancreas, gill, heart, gonad, stomach) were separated from 15 healthy adult shrimp (approximately 1.5 ± 0.5 cm in length and 70 ± 10 mg in weight) and stored at −80 °C for the next steps. The copper exposure experiment was referred to Xing et al. [35]. and samples were collected at 0, 6, 12, 24, 36, 48, 72 h for RNA extraction.

2.2. RNA isolation and cDNA synthesis

The total RNA of the collected samples was extracted with Trizol® reagent (Thermo, USA) and treated with RQI RNase-Free DNase (Promega, USA) following the manufacturer's instruction. A NanoDrop 2000c (Thermo Scientific, USA) was used to measure the quantity and quality of RNA. Then, 1 μg total RNA was added to synthesize cDNA using HiScript® III 1st Strand cDNA Synthesis Kit (Vazyme, CN) according to the manufacturer's protocol.

Fig. 1. The cDNA and deduced amino acid sequence of NdPrx3. The start (ATG) and stop codons(TAA) are marked with an arrow and "*". The polyadenylation signal (AATAAA) is surrounded by a black rectangular box.

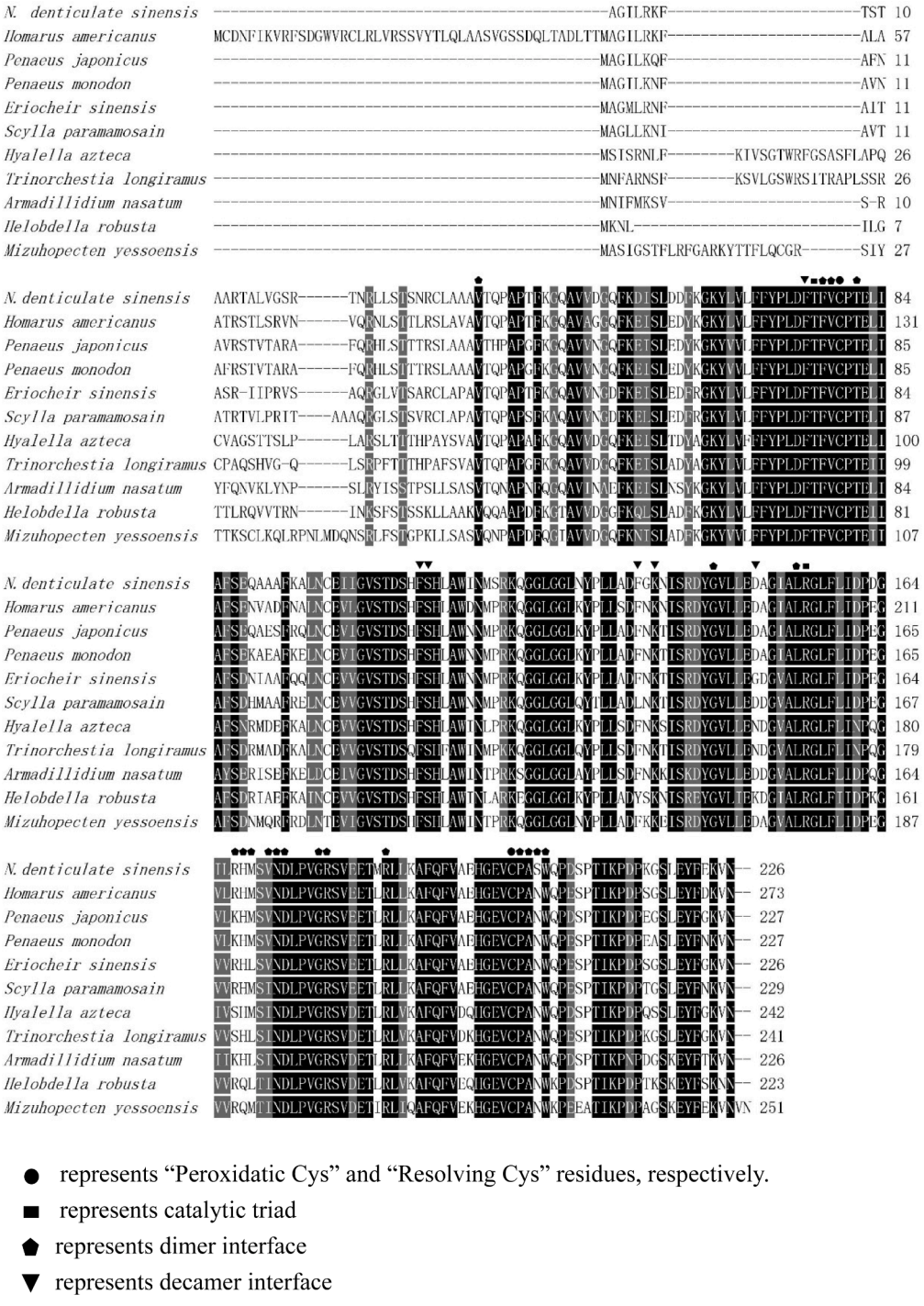

Fig. 2. Multiple sequence alignments of NdPrx3 with others known as Prx3 in many species. The amino acids padded with black were the same and gray was highly conserved.

2.3. Quantitative real-time PCR (qRT-PCR) analysis of NdPrx3

qRT-PCR was used to detect the distribution of *NdPrx3* in different tissues and the expression profiles at copper exposure. 18S rRNA gene was adopted as the reference gene. Primers are shown in Table 1. qRT-PCR was conducted in a total volume of 10 μL, containing 5 μL of Genlous 2 × SYBR Green Fast qPCR Mix (ABclonal Technology, CN), 4.1 μL of nuclease-free water, 0.2 μL of each primer and 0.5 μL of cDNA template. The program of reaction involved 95 °C for 3 min, then 40 cycles of 95 °C for 10 s, 55 °C for 10 s, and 68 °C for 20 s. The relative quantitative method ($2^{-\triangle\triangle CT}$) was used subsequently for data analysis.

2.4. Expression and purification of recombinant protein in E. coli

The nucleic acid sequence of *NdPrx3* was amplified from the cDNA library stored in our laboratory using primers NdPrx3-F, NdPrx3-F_0, and NdPrx3-R (Table 1). The target sequence was ligated into the pMD®19-T vector. The product pMD-19T-*NdPrx3* was transformed into *E. coli* DH5α. The plasmid was extracted and verified by sequencing. Subsequently, the sequence encoding the mature peptide of NdPrx3 was

Table 2
Result of Blastp by amino acid sequence.

No	Species name	NCBI Accession number	Identity (%)	Query cover (%)	No. of amino acids
1	*Homarus americanus*	XP_042239359	82.30	99	273
2	*Penaeus japonicus*	XP_042874112	80.97	99	227
3	*Penaeus monodon*	XP_037784347	80.97	99	227
4	*Eriocheir sinensis*	QIX12308	79.20	99	226
5	*Portunus trituberculatus*	XP_045119771	78.95	99	229
6	*Procambarus clarkii*	XP_045620436	78.32	99	228
7	*Scylla paramamosain*	ASS34530	77.19	99	229
8	*Hyalella azteca*	XP_018020907	74.43	94	242
9	*Helobdella robusta*	XP_009031320	72.51	92	223
10	*Trinorchestia longiramus*	KAF2357233	75.36	91	241

seamlessly cloned into the plasmid pCT7-CHISP6H constructed by our laboratory [36] and transformed into *E. coli* BL21 for expression induced by IPTG. The product was detected by SDS-PAGE using 15% separating gel and 5% (w/v) stacking gel and purified by Ni-NTA-agarose resin [37].

2.5. Enzymatic assay for recombinant NdPrx3 activities

The *E. coli* BL21 was collected by centrifugation at 5000 rpm for 20 min after induction of expression by IPTG. The supernatant was poured out and buffer PBS was added for ultrasonic crushing. The supernatant was collected by centrifugation and crude enzyme solution was obtained. The concentration of total protein in crude enzyme solution was determined by NanoDrop 2000c (Thermo Scientific, USA).

The peroxidase activity assay of *NdPrx3* crude enzyme solution was determined by Catalase Assay Kit (Beyotime S0051, CN) according to the manual. *E. coli* BL21 cells which transformed into a plasmid encoding recombinant lipase was used as a negative control. Double distilled water was used as a blank. Additionally, the thermal stability was analyzed by measuring the reduction of hydrogen peroxide at different temperatures (from 10 °C to 70 °C).

2.6. DNA protecting activity of NdPrx3

The Mixed-Function Oxidase (MFO) assay was used to detect the DNA protecting activity of r*NdPrx3* from oxidative challenge [38,39]. The MFO Mix (3.3 mM DTT, 16.5 μM $FeCl_3$, and H_2O) was incubated with varying concentrations of *rNdPrx3* at 37 °C for 1.5 h. Thereafter, pUC19 DNA was added and incubated at 37 °C for 2 h. Bovine serum albumin (BSA) was used as the control group. Finally, Samples were subjected to 1% agarose gel by electrophoresis at 100 mV for 25 min. The agarose gel was visualized under UV light.

2.7. Bioinformatic analysis

The cDNA sequence of *NdPrx3* was identified from the *N. denticulata sinensis* transcriptome database constructed by our laboratory by using the Basic Local Alignment Search Tool (BLAST) downloaded from NCBI (https://blast.ncbi.nlm.nih.gov/Blast.cgi). SignalP 5.0 was used to detect the excision of signal peptide (https://services.healthtec h.dtu. d k/servi ce.php? Si gnalP-5.0). The conserved domains of the amino acid sequence were predicted using NCBI conserved domain database (https://www.ncbi.nlm.nih.gov/Structure/cdd/wrpsb.cgi) and ExPASy PROSITE database (https://prosite.expasy.org/) [26]. MW and pI were predicted by Expasy Compute pI/Mw (https://web.expasy.org/compute_pi/). The similarity of the amino acid sequence of NdPrx3 was determined by the online BLAST of NCBI (https://blast.ncbi.nlm.nih.gov/Blast.cgi). Multiple sequence alignments were based on local MAFFT 7 downloaded from (https://mafft.cbrc.jp/alignment/software/) [40]. Color Align Conservation Tool of Sequence Manipulation Suite was used to fill the conserved area (http://www.bioinformatics.org/sms2/color_align_cons.html). The phylogenetic tree was built using the Neighbor-Joining method with 5000 bootstraps in MEGA 11.0 software.

2.8. Statistical analysis

The results of qPCR experiments and peroxidase activity detection were analyzed with three parallel groups and presented as mean ± standard deviation (SD). The significance ($P < 0.05$) of qPCR assays and peroxidase activity detection was analyzed by one-way analysis of variance (ANOVA) using GraphPad Prism and SPSS Statistics 19.0 software (IBM Corporation, USA), respectively.

3. Results

3.1. Characterization of NdPrx3

According to the transcriptomic database and genomic database constructed by our laboratory, the full-length cDNA sequence (named *NdPrx3*) was obtained with 1098 bp (GenBank accession no. OM678462). As shown in Fig. 1, the complete nucleotide sequence of *NdPrx3* contained a 684 bp open reading frame (ORF), a 213 bp 5′ untranslated region and a 201 bp 3′ untranslated region. The ORF encoded NdPrx3 of 227 amino acids with a predicted molecular weight (MW) about 24.7 kDa and theoretical isoelectric point (pI) of 6.49 (Fig. 1). Conserved domain prediction revealed that NdPrx3 was a group of Typical 2-Cys-Prx subfamily, thioredoxin_ like superfamily. The peroxidatic and resolving cysteines were located at Cys^{79} in N-terminal and Cys^{200} in C-terminal, respectively. The catalytic triad was present at residues Thr^{76}, Cys^{79}, and Arg^{155}. The dimer interface included 19 amino acid residues: Val^{36}, Phe^{77}, Val^{78}, Thr^{81}, Gly^{144}, Leu^{154}, Arg^{167}, His^{168}, Met^{169}, Val^{171}, Asn^{172}, Asp^{173}, Gly^{177}, Arg^{178}, Arg^{185}, Cys^{200}, Pro^{201}, Ala^{202}, Ser^{203}. The decamer interface was located at Phe^{75}, Phe^{109}, Ser^{110}, Phe^{135}, Lys^{137}, Asp^{149} (Fig. 2).

The highest identity (82.30%) and Query Cover (99%) during the result of BLAST online was Thioredoxin-dependent peroxide reductase of *Homarus americanus* (Table 2). The phylogenetic tree was constructed using the amino acid sequence of the 42 sequences that came from different subfamilies of Prxs. Branches were divided into six groups representing different Peroxidases (Prx 1 to Prx 6) and NdPrx3 belonged to the Prx3 branch (Fig. 3). Combined with previous studies described in the introduction, the tree clearly showed that atypical Prxs (Prx5) has more difference with another two groups compared with 1-Cys-Prxs (Prx6) and typical 2-Cys-Prxs (Prx1–4). In typical Prxs, Prx1, Prx2, and Prx4 have high homology and are significantly different from Prx3. We considered that was because Prx3 only presents in mitochondria.

3.2. Distribution of NdPrx3 mRNA in different tissues

The mRNA expression of *NdPrx3* was detected in different tissues separated from healthy shrimp by quantitative real-time PCR. The result showed that the relative expression level in the gill was the highest and followed by eyestalk. Cuticle and muscle had a low relative expression level. There is almost no expression in heart, hepatopancreas, stomach, intestine, and gonad (Fig. 4).

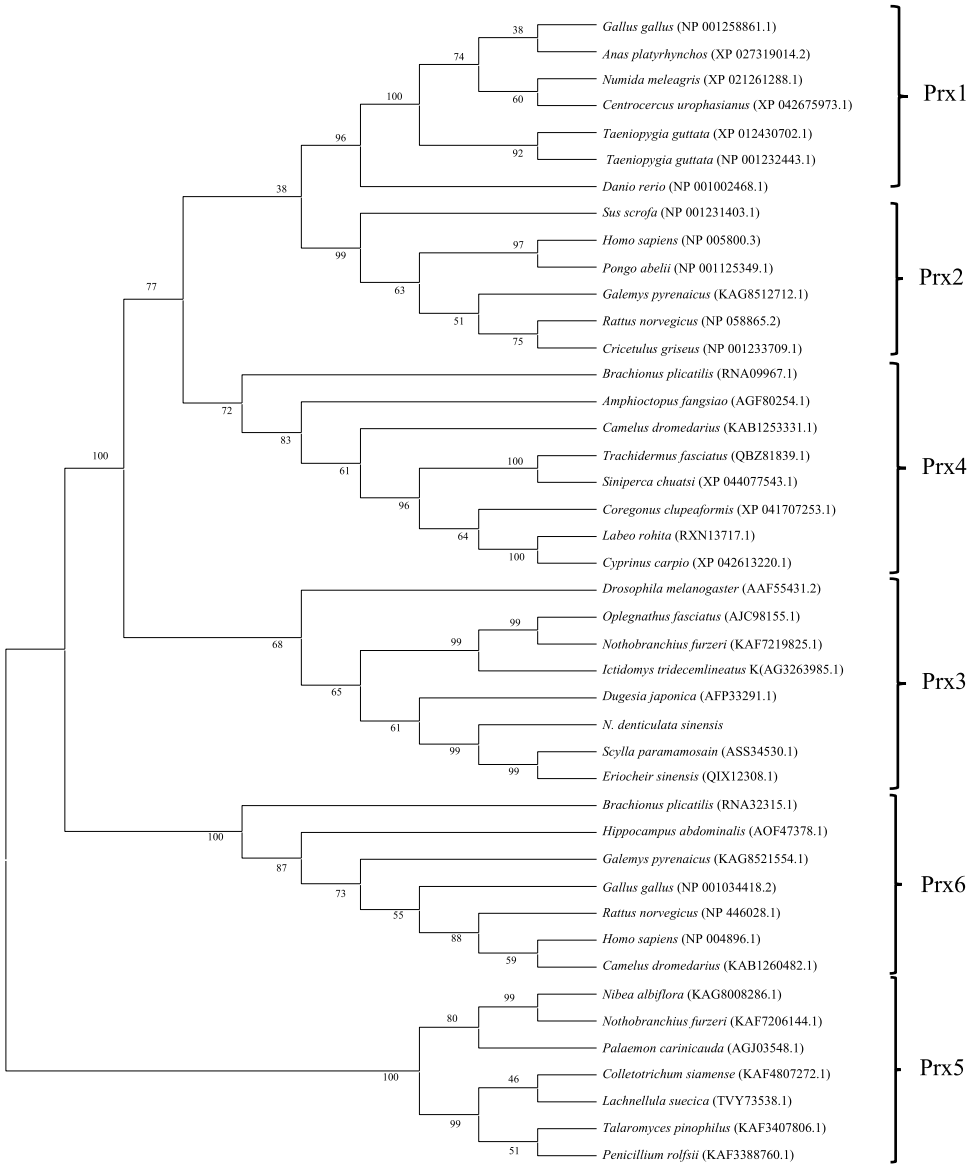

Fig. 3. Phylogenetic analysis of NdPrx3 with other Prxs. MAFFT was used to sequence align and the image was constructed by MEGA 11 with the Neighbor-joining method. The bootstrap replication was 5000 and bootstrap values are marked on the branches. NdPrx3 is surrounded by a black rectangular box. The gene bank accession numbers of these sequences are recorded in rackets.

3.3. Expression profiles of NdPrx3 after the shrimp was challenged with copper exposure

The relative expression of *NdPrx3* mRNA was examined at different time intervals. The relative expression in 0 h was used as the control group in each time interval. The copper exposure experiment showed upregulation of *NdPrx3* from 0 to 48 h and reached the highest at 48 h. Subsequently, there was a significant decrease ($P < 0.01$) from 48 to 72 h (Fig. 5).

3.4. Recombinant expression and purification of NdPrx3

Recombinant NdPrx3 was induced to express in *E. coli* BL21 cells. A pre-experiment with 5 mL LB was used to verify the expression of recombinant NdPrx3. Samples were taken every two hours during the 6-hour IPTG induction. The purified protein was visualized as a single band by SDS-PAGE (Fig. 6). The actual size of the NdPrx3 protein was close to the predicted MW.

3.5. Enzymatic activity of recombinant NdPrx3

The total protein concentration of the crude protein solution was 35.74 mg/mL. In the system specified of the kit, a total of 0.00223 μmol hydrogen peroxide was reduced in 1 min. According to the formula provided in the manual, the enzyme activity of recombinant NdPrx3 was 278.75 units/mL at 25 °C (pH 7.0). There was no significant reduction between negative control (N) and blank control (B) (Fig. 7). Additionally, they were both significantly different from the treatment group (T).

According to the result of stability of recombinant NdPrx3, it had a stable activity in the range of 10 °C to 30 °C. The activity of rNdPrx3 decreased with increasing temperature after 30 °C illustrating that it was less stable at high temperatures (Fig. 8).

3.6. DNA protecting activity of rNdPrx3

We determined the DNA protecting activity of rNdPrx3 using the MFO assay with pUC19 plasmid. As shown in Fig. 9, MFO broke the

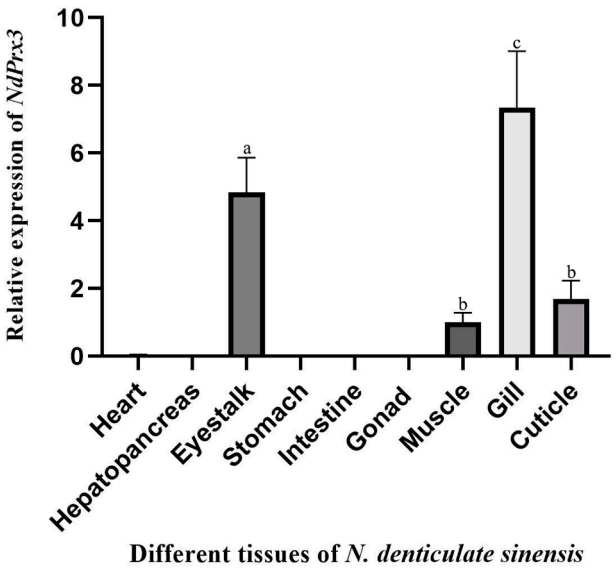

Fig. 4. The mRNA expression profile of *NdPrx3*. Relative expression was calculated with the $2^{-\triangle\triangle CT}$ method using the 18S rRNA gene as the internal control. The significant difference in fold values ($P < 0.05$) was marked on the error bars according to the result of multiple comparisons.

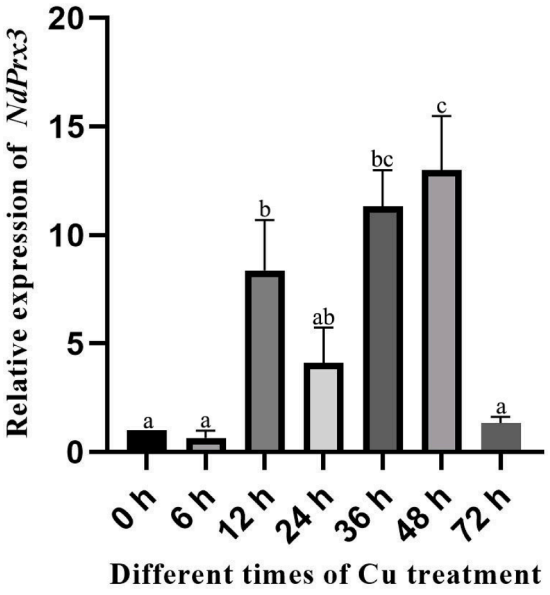

Fig. 5. The mRNA expression profile of *NdPrx3* after copper challenge. The reaction was performed at different times (0 h, 6 h, 12 h, 24 h, 36 h, 48 h, 72 h). The significant difference in fold values ($P < 0.05$) was marked on the error bars according to the result of multiple comparisons.

supercoiled plasmid and formed nicked DNA. Compared to the normal band the nicked DNA was behind. The result showed that rNdPrx3 has a DNA-protecting function which is correlated with rNdPrx3 concentration in the range of protein concentration used in this experiment (Lines 4 to 8). In addition, the negative control (Lines 2 and 3) illustrated no other interference.

4. Discussion

According to the previous studies, the Prx family was divided into six subfamilies (Prx 1–6), and Prx3 participated in the reduction of mitochondrial peroxide levels. Mitochondria is the mainly aerobic breathing place. Energy generation is accompanied by many reactive oxygen species (ROS) [41]. Prx3 is one of the regulators of the balance between generation and reduction of ROS in mitochondria. The identified *NdPrx3* cDNA sequence contained 684 bp ORF which encoded 24.7 kDa protein within the average size (20–30 kDa) of Prxs [42]. Prediction and comparison results of NdPrx3 conserve domain showed it is most common with some reported Prx3 in crustaceans, including *H. americanus* [43], *Scylla paramamosain* [44], *Trinorchestia longiramus* [45], and *Armadillidium nasatum* [46]. For its existence in mitochondria, the homology of Prx3 was high in different species.

Adjacent to the peroxidatic cysteine residues (Cys^{79}) was an active site motif "72-PLDFTFVC-79" which was concluded as a universal active site structure ($PXXXTXXC_P$) of Prxs [7]. The peroxidatic and resolving cysteine residues (Cys^{79}, Cys^{200}) of *NdPrx3* were the characteristic feature of typical 2-Cys-indicating that it belongs to the typical 2-Cys-Prx subfamily. Other special structures of Prxs including catalytic triad, dimer, and decamer interfaces were also identified in *NdPrx3*.The phylogenetic relationship demonstrated that NdPrx3 clustered in the Prx3 class further indicating that NdPrx3 is closely related to Prx3.

The distribution of *NdPrx3* mRNA was detected in nine tissues of unchallenged shrimps by real-time PCR, and the two organizations (gill and eyestalk) with higher relative expression were found. Muscle and cuticle displayed a lower expression level. But the relative expression of NdPrx3 in muscles with more energy consumption was much lower than that in gills which was similar to that in *O. fasciatus* [25]. There is almost no relative expression of other tissues including the heart, hepatopancreas, stomach, intestine, and gonad. The gills of shrimp have great importance in their life for taking on the functions of breathing and filtering the impurities in water. So, gills have more chance of exposure to pathogens [47]. In addition, Prx family members are also known as a process of the immune mechanism against a variety of bacteria and viruses. Gills require a lot of energy to maintain the body's survival and also undertake the function of immunity, so it has a high NdPrx3 expression level. In previous studies, Yang et al. [27] and Samaraweera et al. [26] reported that Prx3 of *C. carpio* and *H. abdominalis* had enriched in the gonad among the species they studied, but in research of *O. fasciatus* [25] and *Miichthys miiuy* [48], they were highest in the liver. In our previous work, we found that the ovary was at a relatively low level of *NdPrx3* expression, probably caused by the different stages of ovarian development.

Copper ions are harmful to organisms because they can snatch electrons to form ROS that causes oxidative damage to tissues [49]. Prxs should be considered as modulators of ROS, so the copper expose experiment can examine the function of *NdPrx3*. After copper exposure, the relative expression of *NdPrx3* gradually rises over 0–48 h. The phenomenon that no significant change in 0–6 h and a significant increase in 6–12 h probably because cells were adapting to the challenging environment. Then the relative expression level was significantly increased illustrating that *NdPrx3* is a strategy of shrimp to prevent cells from oxidative damage. In this experiment, the method of copper exposure was creating a water environment rich in copper ions [35], so gill and eyestalk were the first two tissues that contacted the copper ions. Meanwhile, the expression of *NdPrx3* had also increased to protect cells. Currently, studies surrounding the Prx3 genes in crustaceans were not a lot and most of them focus on the effect of pathogen challenge on the Prx3 expression, while a few research on the challenge by heavy metal ions. In addition, the injection method may produce different results than the method used in this paper.

Previous work showed that excessive ROS in biological organizes may damage the macromolecules, including lipids, proteins, and DNA [50]. In this study, DNA protecting activity of rNdPrx3 was examined using MFO assay. Line 2 of Fig. 9 showed that the MFO system still produces enough ROS to break supercoiled DNA as predicted though we changed the volumes of each component in the system compared with

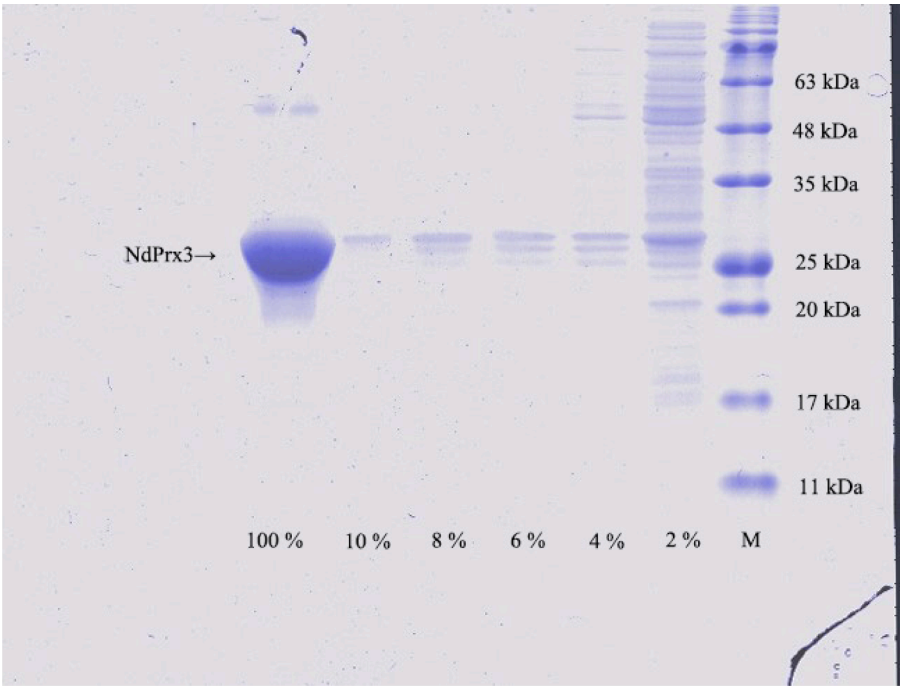

Fig. 6. The protein purification of NdPrx3 in SDS-PAGE. M represents the protein ladder. Followed lanes are low-concentration imidazole solution flow-through (2%, 4%, 6%, 8%, 10%). The 100% lane is purified NdPrx3 protein (24.7 kDa).

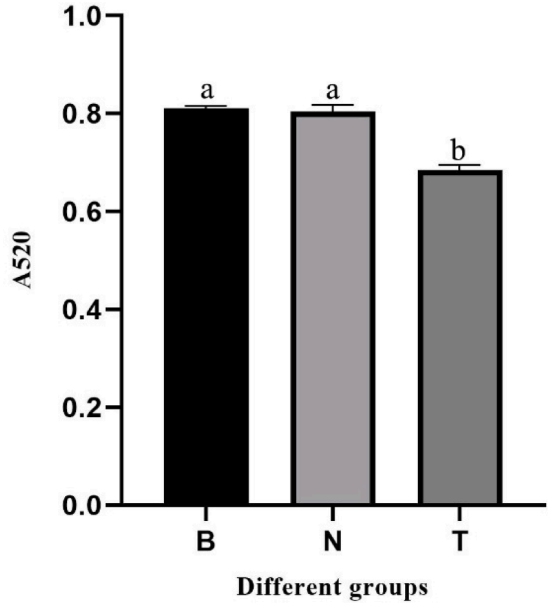

Fig. 7. The absorbance of different groups at 520 nm wavelength. B represents blank control used dd H_20. N was negative control used a recombinant lipase. T was the treatment group with *NdPrx3*. The significant difference in fold values ($P < 0.05$) was marked on the error bars according to the result of ANOVA by SPSS Statistics 19 software.

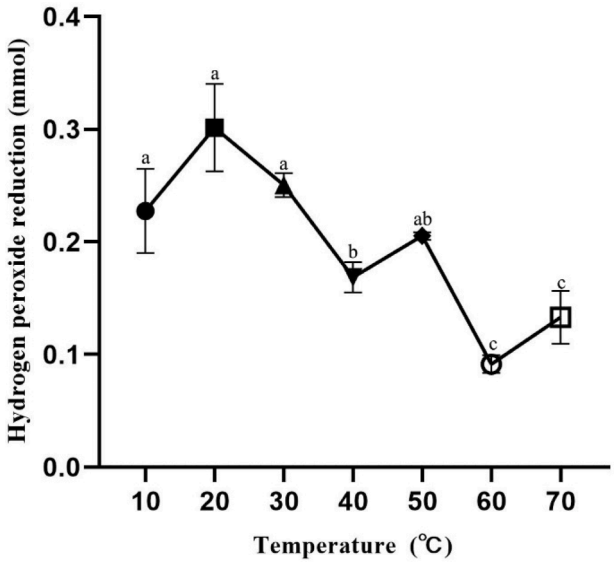

Fig. 8. Influence of temperature on enzymatic activity of rNdPrx3. The significant difference in fold values ($P < 0.05$) was marked on the error bars according to the result of multiple comparisons.

Cheng`s work. This suggests that rNdPrx3 can also neutralize the oxidative damage caused by copper ions rather than the effects of free radicals produced by cellular respiration. Our study supports this point of view that Prx3 is considered the modulator of the DNA damage caused by ROS and plays an important role when aquatic organisms face oxidative damage.

In conclusion, the putative cDNA sequence of *N. denticulata sinensis* was identified and cloned, and the distribution of NdPrx3 mRNA in various tissues was detected. The recombinant NdPrx3 was successfully expressed by constructing plasmids and transforming *E. coli* BL21. The enzyme activity and the peroxidase assay suggested the function of recombinant NdPrx3 in hydrogen peroxide removal. Its role in immunity against pathogenic infection mentioned in related studies is needed to clarify and analyze in the future.

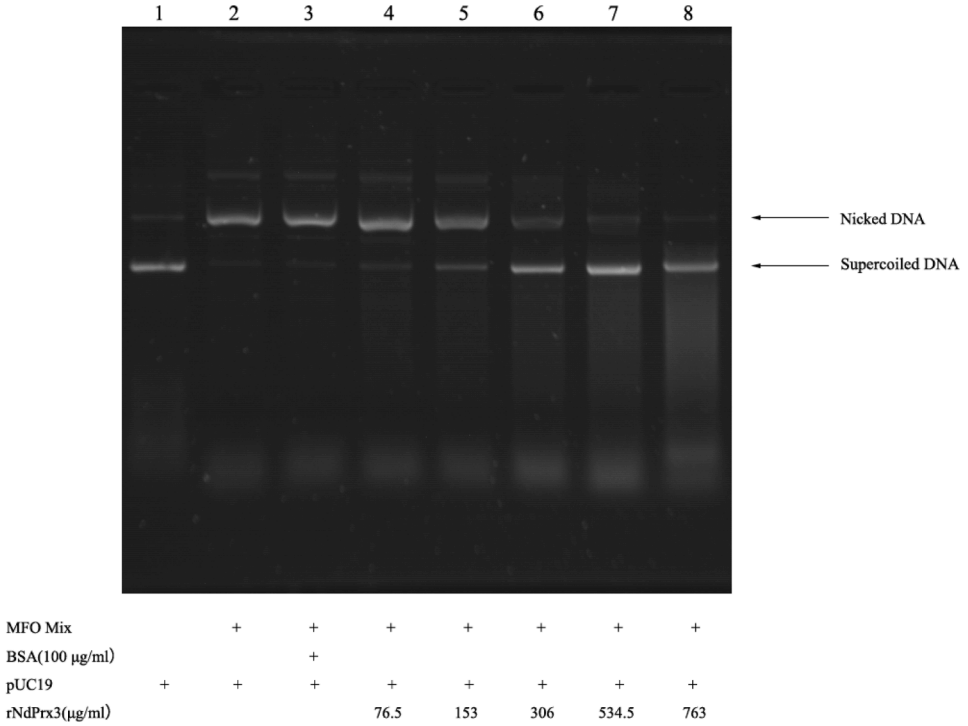

Fig. 9. Protection of supercoiled DNA cleavage by *rNdPrx3* in MFO system. The total volume of system was 20 μL contained plasmid (5 μL), protein (2 μL), MFO Mix (2 μL), and H_2O. 1: pUC19 (224.7 ng/μL) + H_2O; 2: pUC19 + MFO Mix + H_2O; 3: pUC19 + MFO Mix + BSA (100 μg/mL); 4: pUC19 + MFO Mix +*rNdPrx3* (76.5 μg/mL); 5: pUC19 + MFO Mix +*rNdPrx3* (153 μg/mL); 6: pUC19 + MFO Mix +*rNdPrx3* (306 μg/mL); 7: pUC19 + MFO Mix +*rNdPrx3* (534.5 μg/mL); 8: pUC19 + MFO Mix +*rNdPrx3* (763 μg/mL).

Declaration of Competing Interest

There is no conflict of interest.

Data availability

No data was used for the research described in the article.

Acknowledgments

This work was supported by the National Natural Science Foundation of China (Grant Nos. 32172954, 41876196, 31872613), and Hangzhou Qianjiang Special Expert for Prof. Jiquan Zhang.

References

[1] K. Kim, I.H. Kim, K.Y. Lee, S.G. Rhee, E.R. Stadtman, The isolation and purification of a specific "protector" protein which inhibits enzyme inactivation by a thiol/Fe (III)/O2 mixed-function oxidation system, J. Biol. Chem. 263 (10) (1988) 4704–4711, https://doi.org/10.1016/s0021-9258(18)68840-4.

[2] H.Z. Chae, S.J. Chung, S.G. Rhee, Thioredoxin-dependent peroxide reductase from yeast, J. Biol. Chem. 269 (44) (1994) 27670–27678, https://doi.org/10.1016/s0021-9258(18)47038-x.

[3] H.Z. Chae, K. Robison, L.B. Poole, G. Church, G. Storz, S.G. Rhee, Cloning and sequencing of thiol-specific antioxidant from mammalian brain: alkyl hydroperoxide reductase and thiol-specific antioxidant define a large family of antioxidant enzymes, Proc. Natl. Acad. Sci. U. S. A. 91 (15) (1994) 7017–7021, https://doi.org/10.1073/pnas.91.15.7017.

[4] L.A. Tartaglia, G. Storz, M.H. Brodsky, A. Lai, B.N. Ames, Alkyl hydroperoxide reductase from *Salmonella typhimurium*. Sequence and homology to thioredoxin reductase and other flavoprotein disulfide oxidoreductases, J. Biol. Chem. 265 (18) (1990) 10535–10540.

[5] W.A. Pushpamali, M. De Zoysa, H.S. Kang, C.H. Oh, I. Whang, S.J. Kim, J. Lee, Comparative study of two thioredoxin peroxidases from disk abalone (*Haliotis discus discus*): cloning, recombinant protein purification, characterization of antioxidant activities and expression analysis, Fish Shellfish Immunol. 24 (3) (2008) 294–307, https://doi.org/10.1016/j.fsi.2007.11.016.

[6] S.G. Rhee, S.W. Kang, T.S. Chang, W. Jeong, K. Kim, Peroxiredoxin, a novel family of peroxidases, IUBMB Life 52 (1–2) (2001) 35–41, https://doi.org/10.1080/15216540252774748.

[7] S.G. Rhee, Overview on peroxiredoxin, Mol. Cells 39 (1) (2016) 1–5, https://doi.org/10.14348/molcells.2016.2368.

[8] Z.A. Wood, E. Schroder, J. Robin Harris, L.B. Poole, Structure, mechanism and regulation of peroxiredoxins, Trends Biochem. Sci. 28 (1) (2003) 32–40, https://doi.org/10.1016/s0968-0004(02)00003-8.

[9] L.B. Poole, The catalytic mechanism of peroxiredoxins, Subcell. Biochem. 44 (2007) 61–81.

[10] A.V. Peskin, C.C. Winterbourn, The enigma of 2-Cys peroxiredoxins: what are their roles? Biochemistry 86 (1) (2021) 84–91, https://doi.org/10.1134/S0006297921010089. -Moscow+.

[11] T.J. Jonsson, W.T. Lowther, The peroxiredoxin repair proteins, Subcell. Biochem. 44 (2007) 115–141, https://doi.org/10.1007/978-1-4020-6051-9_6.

[12] A. Hall, P.A. Karplus, L.B. Poole, Typical 2-Cys peroxiredoxins–structures, mechanisms and functions, FEBS J. 276 (9) (2009) 2469–2477, https://doi.org/10.1111/j.1742-4658.2009.06985.x.

[13] K.S. Yang, S.W. Kang, H.A. Woo, S.C. Hwang, H.Z. Chae, K. Kim, S.G. Rhee, Inactivation of human peroxiredoxin I during catalysis as the result of the oxidation of the catalytic site cysteine to cysteine-sulfinic acid, J. Biol. Chem. 277 (41) (2002) 38029–38036, https://doi.org/10.1074/jbc.M206626200.

[14] M.I. De Armas, R. Esteves, N. Viera, A.M. Reyes, M. Mastrogiovanni, T.G.P. Alegria, L.E.S. Netto, V. Tortora, R. Radi, M. Trujillo, Rapid peroxynitrite reduction by human peroxiredoxin 3: implications for the fate of oxidants in mitochondria, Free Radic. Bio Med. 130 (2019) 369–378, https://doi.org/10.1016/j.freeradbiomed.2018.10.451.

[15] M.A. Packer, C.M. Porteous, M.P. Murphy, Superoxide production by mitochondria in the presence of nitric oxide forms peroxynitrite, Biochem. Mol. Biol. Int. 40 (3) (1996) 527–534, https://doi.org/10.1080/15216549600201103.

[16] M.N. Abbas, S. Kausar, H.J. Cui, The biological role of peroxiredoxins in innate immune responses of aquatic invertebrates, Fish Shellfish Immunol. 89 (2019) 91–97, https://doi.org/10.1016/j.fsi.2019.03.062.

[17] S.G. Rhee, I.S. Kil, Multiple functions and regulation of mammalian peroxiredoxins, Annu. Rev. Biochem. 86 (2017) 749–775, https://doi.org/10.1146/annurev-biochem-060815-014431.

[18] T.E. Forshaw, R. Holmila, K.J. Nelson, J.E. Lewis, M.L. Kemp, A.W. Tsang, L. B. Poole, W.T. Lowther, C.M. Furdui, Peroxiredoxins in cancer and response to radiation therapies, Antioxidants 8 (1) (2019), 8010011, https://doi.org/10.3390/antiox8010011. -Basel.

[19] T.S. Chang, W. Jeong, S.Y. Choi, S. Yu, S.W. Kang, S.G. Rhee, Regulation of peroxiredoxin I activity by Cdc2-mediated phosphorylation, J. Biol. Chem. 277 (28) (2002) 25370–25376, https://doi.org/10.1074/jbc.M110432200.

[20] H.A. Woo, S.H. Yim, D.H. Shin, D. Kang, D.Y. Yu, S.G. Rhee, Inactivation of peroxiredoxin I by phosphorylation allows localized H(2)O(2) accumulation for cell signaling, Cell 140 (4) (2010) 517–528, https://doi.org/10.1016/j.cell.2010.01.009.

[21] A. Perkins, L.B. Poole, P.A. Karplus, Tuning of peroxiredoxin catalysis for various physiological, Biochemistry 53 (49) (2014) 7693–7705, https://doi.org/10.1021/bi5013222. -Us.

[22] L. van Dam, M. Pages-Gallego, P.E. Polderman, R.M. van Es, B.M.T. Burgering, H. R. Vos, T.B. Dansen, The human 2-Cys peroxiredoxins form widespread, Cysteine-dependent- and isoform-specific protein-protein interactions, Antioxidants (Basel) 10 (4) (2021), 10040627, https://doi.org/10.3390/antiox10040627.
[23] G.I. Godahewa, N.C.N. Perera, J. Lee, Insights into the multifunctional role of natural killer enhancing factor-A (NKEF-A/Prx1) in big-belly seahorse (*Hippocampus abdominalis*): DNA protection, insulin reduction, H2O2 scavenging, and immune modulation activity, Gene 642 (2018) 324–334, https://doi.org/10.1016/j.gene.2017.11.042.
[24] M. De Zoysa, J.H. Ryu, H.C. Chung, C.H. Kim, C. Nikapitiya, C. Oh, H. Kim, K. S. Revathy, I. Whang, J. Lee, Molecular characterization, immune responses and DNA protection activity of rock bream (*Oplegnathus fasciatus*), peroxiredoxin 6 (Prx6), Fish Shellfish Immunol. 33 (1) (2012) 28–35, https://doi.org/10.1016/j.fsi.2012.03.029.
[25] G.I. Godahewa, Y. Kim, S.H.S. Dananjaya, R.G.P.T. Jayasooriya, J.K. Noh, J. Lee, M. De Zoysa, Mitochondrial peroxiredoxin 3 (Prx3) from rock bream (*Oplegnathus fasciatus*): immune responses and role of recombinant Prx3 in protecting cells from hydrogen peroxide induced oxidative stress, Fish Shellfish Immunol. 43 (1) (2015) 131–141, https://doi.org/10.1016/j.fsi.2014.12.011.
[26] A. Vidurangi Samaraweera, M.D. Neranjan Tharuka, T. Thiunuwan Priyathilaka, H. Yang, S. Lee, J. Lee, Molecular profiling and functional delineation of peroxiredoxin 3 (HaPrx3) from the big-belly seahorses (*Hippocampus abdominalis*) and understanding their immunological responses, Gene 771 (2021), 145350, https://doi.org/10.1016/j.gene.2020.145350.
[27] Y.Z. Yang, Y. Zhao, L. Yang, L.P. Yu, H. Wang, X.S. Ji, Characterization of 2-Cys peroxiredoxin 3 and 4 in common carp and the immune response against bacterial infection, Comp. Biochem. Phys. B 217 (2018) 60–69, https://doi.org/10.1016/j.cbpb.2017.12.012.
[28] Y. Liu, K. Xing, C. Yan, Y. Zhou, X. Xu, Y. Sun, J. Zhang, Transcriptome analysis of Neocaridina denticulate sinensis challenged by Vibrio parahemolyticus, Fish Shellfish Immunol. 121 (2021) 31–38, https://doi.org/10.1016/j.fsi.2021.10.004.
[29] D.J. Huang, H.C. Chen, J.P. Wu, S.Y. Wang, Reproduction obstacles for the female green neon shrimp (*Neocaridina denticulata*) after exposure to chlordane and lindane, Chemosphere 64 (1) (2006) 11–16, https://doi.org/10.1016/j.chemosphere.2005.12.017.
[30] C.H. Tang, W.Y. Chen, C.C. Wu, E. Lu, W.Y. Shih, J.W. Chen, J.W. Tsai, Ecosystem metabolism regulates seasonal bioaccumulation of metals in atyid shrimp (*Neocaridina denticulata*) in a tropical brackish wetland, Aquat. Toxicol. 225 (2020), 105522, https://doi.org/10.1016/j.aquatox.2020.105522.
[31] C.W. Oh, C.W. Ma, R.G. Hartnoll, H.L. Suh, Reproduction and population dynamics of the temperate freshwater shrimp, Neocaridina denticulata denticulata (De Haan, 1844), in a Korean stream, Crustaceana 76 (2003) 993–1015, https://doi.org/10.1163/156854003771997864.
[32] Y. Huang, L. Zhang, G. Wang, S. Huang, *De novo* assembly transcriptome analysis reveals the genes associated with body color formation in the freshwater ornamental shrimps *Neocaridina denticulate sinensis*, Gene 806 (2022), https://doi.org/10.1016/j.gene.2021.145929.
[33] D.L. Mykles, J.H.L. Hui, *Neocaridina denticulata*: a Decapod crustacean model for functional genomics, Integr. Comp. Biol. 55 (5) (2015) 891–897, https://doi.org/10.1093/icb/icv050.
[34] N. Niwa, M. Ueno, Y. Inoue, Accumulation of trypan blue and trypan red in nephrocytes of the fresh-water shrimp *Neocaridina denticulata* (decapoda: atyidae), J. Crustacean Biol. 18 (4) (1998) 666–672, https://doi.org/10.2307/1549141.
[35] K. Xing, Y. Liu, C. Yan, Y. Zhou, Y. Sun, N. Su, F. Yang, S. Xie, J. Zhang, Transcriptome analysis of Neocaridina denticulate sinensis under copper exposure, Gene 764 (2021), 145098, https://doi.org/10.1016/j.gene.2020.145098.
[36] Y.Y. Sun, J.Q. Zhang, S.J. Wang, Heterologous expression and efficient secretion of chitosanase from *Microbacterium sp* in *Escherichia coli*, Indian J. Microbiol. 55 (2) (2015) 194–199, https://doi.org/10.1007/s12088-014-0505-5.
[37] M. Li, X.Y. Wang, J.G. Bai, Purification and characterization of arginine kinase from locust, Protein Pept. Lett. 13 (4) (2006) 405–410, https://doi.org/10.2174/092986606775974375.
[38] D. Cheng, H. Zhang, H. Liu, X. Zhang, K. Tan, S. Li, H. Ma, H. Zheng, Identification and molecular characterization of peroxiredoxin 6 from noble scallop *Chlamys nobilis* revealing its potent immune response and antioxidant property, Fish Shellfish Immunol. 100 (2020) 368–377, https://doi.org/10.1016/j.fsi.2020.03.021.
[39] S.H. Chu, L. Liu, M.N. Abbas, Y.Y. Li, S. Kausar, X.Y. Qian, Z.Z. Ye, X.M. Yu, X.K. Li, M. Liu, L.S. Dai, Peroxiredoxin 6 modulates Toll signaling pathway and protects DNA damage against oxidative stress in red swamp crayfish (*Procambarus clarkii*), Fish Shellfish Immunol. 89 (2019) 170–178, https://doi.org/10.1016/j.fsi.2019.03.055.
[40] K. Katoh, K. Misawa, K. Kuma, T. Miyata, MAFFT: a novel method for rapid multiple sequence alignment based on fast Fourier transform, Nucleic Acids Res. 30 (14) (2002) 3059–3066, https://doi.org/10.1093/nar/gkf436.
[41] T. Ismail, Y. Kim, H. Lee, D.S. Lee, H.S. Lee, Interplay between mitochondrial peroxiredoxins and ROS in cancer development and progression, Int. J. Mol. Sci. 20 (18) (2019), 20184407, https://doi.org/10.3390/ijms20184407.
[42] Y. Valero, F.J. Martinez-Morcillo, M.A. Esteban, E. Chaves-Pozo, A. Cuesta, Fish peroxiredoxins and their role in immunity, Biology (Basel) 4 (4) (2015) 860–880, https://doi.org/10.3390/biology4040860.
[43] A.E. Christie, M. Chi, T.J. Lameyer, M.G. Pascual, D.N. Shea, M.E. Stanhope, D. J. Schulz, P.S. Dickinson, Neuropeptidergic signaling in the American lobster *Homarus americanus*: new insights from high-throughput nucleotide sequencing, PLoS One 10 (12) (2015), 0145964, https://doi.org/10.1371/journal.pone.0145964.
[44] D.D. Tu, Y.L. Zhou, W.B. Gu, Q.H. Zhu, B.P. Xu, Z.K. Zhou, Z.P. Liu, C. Wang, Y. Y. Chen, M.A. Shu, Identification and characterization of six peroxiredoxin transcripts from mud crab Scylla paramamosain: the first evidence of peroxiredoxin gene family in crustacean and their expression profiles under biotic and abiotic stresses, Mol. Immunol. 93 (2018) 223–235, https://doi.org/10.1016/j.molimm.2017.11.029.
[45] J. Woo, H. An, B.J. Lim, H.Y. Song, M.S. Kim, T.W. Jung, S. Jeong, I.Y. Cho, S. Oh, D. Han, M. Yoon, Demographic history of *Trinorchestia longiramus* (Amphipoda, Talitridae) in South Korea inferred from mitochondrial DNA sequence variation, Crustaceana 89 (13) (2016) 1559–1573, https://doi.org/10.1163/15685403-00003608.
[46] T. Becking, M.A. Chebbi, I. Giraud, B. Moumen, T. Laverre, Y. Caubet, J. Peccoud, C. Gilbert, R. Cordaux, Sex chromosomes control vertical transmission of feminizing Wolbachia symbionts in an isopod, PLoS Biol. 17 (10) (2019), 3000438, https://doi.org/10.1371/journal.pbio.3000438.
[47] X. Gao, C. He, H. Liu, H. Li, D. Zhu, S. Cai, Y. Xia, Y. Wang, Z. Yu, Intracellular Cu/Zn superoxide dismutase (Cu/Zn-SOD) from hard clam *Meretrix meretrix*: its cDNA cloning, mRNA expression and enzyme activity, Mol. Biol. Rep. 39 (12) (2012) 10713–10722, https://doi.org/10.1007/s11033-012-1962-8.
[48] L.P. Ren, Y.N. Sun, R.X. Wang, T.J. Xu, Gene structure, immune response and evolution: comparative analysis of three 2-Cys peroxiredoxin members of miiuy croaker, *Miichthys miiuy*, Fish Shellfish Immunol. 36 (2) (2014) 409–416, https://doi.org/10.1016/j.fsi.2013.12.014.
[49] R.M. Llanos, J.F. Mercer, The molecular basis of copper homeostasis copper-related disorders, DNA Cell Biol. 21 (4) (2002) 259–270, https://doi.org/10.1089/104454902753759681.
[50] C.A. Juan, J.M. Perez de la Lastra, F.J. Plou, E. Perez-Lebena, The chemistry of reactive oxygen species (ROS) revisited: outlining their role in biological macromolecules (DNA, lipids and proteins) and induced pathologies, Int. J. Mol. Sci. 22 (9) (2021), 22094642, https://doi.org/10.3390/ijms22094642.